

Theoretical Analysis of Diamond Mechanosynthesis. Part III. Positional C₂ Deposition on Diamond C(110) Surface Using Si/Ge/Sn-Based Dimer Placement Tools

Jingping Peng,¹ Robert A. Freitas, Jr.,^{2,*} Ralph C. Merkle,³ James R. Von Ehr,¹
John N. Randall,¹ and George D. Skidmore¹

¹Zyvex Corporation, 1321 North Plano Road, Richardson, TX 75081, USA

²Institute for Molecular Manufacturing, Suite 354, Palo Alto, CA 94301, USA

³Georgia Institute of Technology, Atlanta, GA 30332, USA

This paper extends an ongoing computational and theoretical investigation of the vacuum mechanosynthesis of diamond on a clean C(110) diamond surface from carbon dimer (C₂) precursors, using Si-, Ge-, and Sn-substituted triadamantane-based positionally-controlled DCB6 dimer placement tools. Interactions between the dimer placement tools and the C(110) surface are investigated by means of stepwise *ab initio* molecular dynamics (AIMD) simulations, using Density Functional Theory (DFT) with generalized gradient approximation (GGA), implemented in the VASP software package. The Ge-based tool tip provides better functionality over a wider range of temperatures and circumstances (as compared with the Si or Sn tool tips). The transfer of a single carbon dimer from the Si-based tool tip onto C(110) is not controllable at 300 K but is workable at 80 K; the Ge-based tool remains workable up to 300 K. Geometry optimization suggests the Sn-based tool deposits reliably but the discharged tool is distorted after use; stepwise AIMD retraction simulations (at 300 K for the Sn tip) showed tip distortion with terminating Sn atoms prone to being attracted towards the surface carbon atoms. Stepwise AIMD shows successful placement of a second dimer in a 1-dimer gapped position, and successful intercalation of a third dimer into the 1-dimer gap between two previously deposited dimers, on clean C(110) at 300 K using the Ge tool. Maximum tolerable dimer misplacement error, investigated by stepwise AIMD quantification, is 0.5 Å in *x* (across trough) and 1.0 Å in *y* (along trough) for a positionally-correct isolated C₂ deposition, and 1.0 Å in *x* and 0.3 Å in *y* for C₂ intercalation between two gapped ad-dimers. Rotational misplacement tolerances for dimer placement are ±30° for the isolated dimer and -10°/+22.5° for the intercalated dimer in the *xy* plane, with a maximum tolerable “in plane” tip rolling angle of 32.5° and “out-of-plane” tip rocking angle of 15° for isolated dimer. Classical molecular dynamics (MD) analysis of a new Ge tooltip + handle system at 80 K and 300 K found that dimer positional uncertainty is halved by adding a crossbar in the most compliant direction. We conclude that the Si-based and Ge-based tools can operate successfully at appropriate temperatures, including up to room temperature for the Ge-based tool.

Keywords: Adamantane, AIMD, Carbon, Density Functional Theory, Diamond, Dimer Placement, Germanium, Mechanosynthesis, Nanotechnology, Positional Control, Silicon, Tin, Tooltip, VASP.

1. INTRODUCTION

Merkle and Freitas¹ have proposed the use of Si-, Ge-, Sn-, and Pb-substituted derivatives of the hydrocarbon cage molecule triadamantane as end effectors (placement tools) in an AFM-based nanositioning apparatus for the vacuum mechanosynthesis of diamond nanostructures, via the pick-and-place mechanochemistry of carbon dimers

onto an existing diamond seed cleaved along the C(110) surface plane. With a carbon dimer covalently attached to two terminal Si, Ge or Sn atoms and the substituted triadamantane tooltip (DCB6) either attached to a scanning probe or integrated into an extended diamond lattice, the carbon dimer can be positioned and deposited onto a growing diamond substrate. The success of this process is based on the premise that a typical C–Si, C–Ge or C–Sn bond is weaker than a typical C–C bond^{2,3} and will dissociate

*Author to whom correspondence should be addressed.

first, leaving the carbon dimer covalently attached to the diamond surface.

This paper (Part III) extends an ongoing computational and theoretical investigation of the vacuum mechanosynthesis of diamond on the clean C(110) surface using positionally-constrained carbon dimer (C_2) precursors. Part I provided a detailed atomic picture of the dimer-mediated surface chemistry during the gas-phase growth of dehydrogenated diamond C(110) from C_2 plasmas, deducing some of the many possible stabilized defects that can be formed early in the dimer-mediated diamond growth process.⁴ Part II analyzed the chemical stability and recharging of dimer placement tools from the view of organo-synthesis, presented reaction path potential energy profiles and analysis of a small number of *ab initio* molecular dynamics (AIMD) simulations of tool retraction events, and established preliminary constraints on the required positional precision needed to avoid the formation of stable defects during positional dimer placement to achieve diamond growth.⁵

The present work reports new results of electronic structure geometry optimization and stepwise AIMD simulations of the placement of isolated carbon dimers onto the clean diamond C(110) surface using Si-, Ge-, and Sn-based C_2 dimer placement tools under conditions of constant number of particles (N), volume (V), and temperature (T) (the canonical or constant NVT ensemble), including: (1) studies of deposition and tooltip retraction event sequences; (2) stepwise AIMD simulations of the placement of a second dimer in a gapped position and the subsequent intercalation of a third dimer into the 1-dimer gap between these two previously deposited dimers, on the clean C(110) surface; and (3) stepwise AIMD analysis of the maximum tolerable dimer misplacement errors, both rotational and translational, that will yield a positionally-correct C_2 deposition onto the diamond C(110) surface. The classical molecular dynamics (MD) analysis of temperature effects on the positional uncertainty and control of the terminal carbon dimer for representative tooltips and extended handle structures are also performed in order to aid future specification of experimental protocols to achieve practical diamond mechanosynthesis.

2. COMPUTATIONAL CONSIDERATIONS

Paper II reported our studies, conducted using *ab initio* electronic structure calculations and constant number of atoms, volume, and energy *ab initio* molecular dynamics (AIMD) simulations, of the positionally-controlled placement of C_2 carbon dimers on the clean (dehydrogenated) diamond C(110) surface.⁵ From the reaction path potential energy plots for deposition and retraction of the Si/Ge triadamantane tool, considering that there are two pathways for retraction and assuming the lowest energy reaction pathway would be followed, it was initially concluded that the Si/Ge dimer placement tools would not leave the

terminal carbon dimer bonded to the diamond substrate surface during retraction. A small number of AIMD stepwise simulations were performed to confirm this conclusion and to investigate the effects of internal energy on the tool retraction event. These AIMD simulations were run under conditions of constant number of atoms (N), volume (V), and energy (E) (the microcanonical or constant NVE ensemble) and were initiated at 300 K. The results of the AIMD simulations generally supported the preliminary interpretation from the reaction path potential energy plots, but one of the five AIMD simulations using the Ge tool provided a successful dimer deposition. This left two questions unanswered for future work: (1) whether two pathways must always exist and be accessible during dimer placement tool retraction, and (2) whether an assumption of constant NVE conditions is applicable for AIMD simulations of the real process of deposition/retraction events using a dimer placement tool. In the present work, we address these two outstanding issues and extend previous lines of investigation.

Regarding the first unanswered question, both pathways of the branched mechanosynthetic reaction (i.e., following one pathway the dimer remains on the surface, while following the other pathway the dimer remains on the tool tip) are accessible only if the probabilities of breaking the two C(dimer)–C(surface) bonds and breaking the two C(dimer)–Si/Ge/Sn(tool) bonds are approximately equal during the process, such that the retraction is able to proceed in either direction, leaving the pathway with the lower reaction barrier to dominate. Obviously, the picture of two pathways is oversimplified. The real situation is more complex—as will be seen in the results, the two simplistic pathways do not capture the simulated phenomena well enough. The typical failure event is not an undeposited dimer remaining on the tool tip, but rather is a dimer that has rotated such that one of its carbon atoms remains bonded to the tip with its other carbon atom still bonded to the surface, leaving an unrecoverable situation. During dimer placement tool retraction, the carbon dimer interacts directly with the two corresponding carbon atoms of the surface and the two terminal Si/Ge/Sn atoms of the tool but also with neighboring atoms of both surface and tool. The dimer placement tool retraction is found to be a dynamic and complex process with all atoms vibrating randomly in all directions and constantly changing relative positions, especially in the region of interest (ROI)—in our discussion, the C (surface)–C (dimer)–Si/Ge/Sn (tool) atoms—with net forces that stretch ROI bonds changing during the retraction, and with these forces changing more drastically at higher system temperatures. The analysis provided from a static view of the potential energy curves and from simple theoretical models is therefore not sufficient to predict tool retraction behavior, which requires a dynamic approach. A properly designed *ab initio* molecular dynamics (AIMD) simulation approach

can be used to mimic the real behavior of a system at a specific temperature. To fully simulate a process the speed of real events must be taken into account, but a full AIMD simulation would become an extremely time consuming task, making it impractical to perform complete AIMD calculations in our study. For this reason, the stepwise AIMD simulation was adopted. The stepwise AIMD simulation is not designed to mimic the continuous “real” progress of an event, but rather to check whether or not some phenomenon of interest—say, the breakage of specific bonds—will occur during the progress of an event. Using this method for modeling tooltip retraction, we artificially raise the tool with a reasonable step-size, then fix the positions of some atoms on the top of the tool and perform AIMD simulation under proper conditions for a reasonable period of time with a suitable time-step. The tool displacement step-size should be small enough not to affect the phenomenon of interest, and the simulation time should be long enough to capture the phenomenon of interest. It is of first importance to choose the proper conditions under which such stepwise AIMD simulations are performed.

Regarding the second unanswered question, the choice of using a constant NVT ensemble or a constant NVE ensemble to sample the dimer placement tool retraction process is determined by whether energy can diffuse away from the ROI during the time allowed in a practicable operation. If the practicable retraction speed is quite slow such that any changes in internal energy can be redistributed, letting the system reach equilibrium with the environment, then a constant NVT ensemble is appropriate. If the practicable retraction speed can be extremely fast so that internal energy changes are confined within the ROI, then a constant NVE ensemble should be considered. Comparing the energy transfer speed in the system to the motional speed of a typical scanning tunneling microscope (STM) tip (the closest existing laboratory device to that which might be required to conduct this experiment) provides reasonable justification for using a constant NVT approach. The C–C stretching frequency is about 1200 cm^{-1} , (Ref. [6]) corresponding to $3.6 \times 10^{13}\text{ Hz}$ or a period of vibration of 28 fs. The stretching frequency is $\sim 905\text{ cm}^{-1}$ for C–Si,⁷ a $\sim 37\text{ fs}$ period of vibration, and 708 cm^{-1} or a $\sim 47\text{ fs}$ period for isolated C–Ge dimers.⁷ The energy transfer rate in diamond may be estimated by the acoustic speed in diamond,³ which is $\sim 1.75 \times 10^4\text{ m/s}$ or $\sim 5.7\text{ fs}/\text{\AA}$. Since in an experimental apparatus the vertical movement of an STM tip is typically 1–2 microns per second, equivalent to $\sim 10^{11}\text{ fs}/\text{\AA}$ for lifting a mechanosynthetic tip up or down near the substrate surface, and in no case faster than $\sim 1\text{ mm/sec}$ ($\sim 10^8\text{ fs}/\text{\AA}$), then the practical process of carbon dimer placement tool deposition/retraction can be considered slow enough to keep the system equilibrated with the environment. Therefore, constant NVT conditions should be adopted, not constant NVE conditions, to simulate the real process.

In order to investigate the behaviors of our dimer placement tools based on the above considerations, we performed constant NVT stepwise AIMD simulations on the following systems: Si tooltip retraction at 300 K and 80 K, Si tooltip deposition/retraction at 300 K, Ge tooltip retraction at 300 K, Ge tooltip deposition/retraction at 300 K, and Sn tooltip deposition/retraction at 300 K, all on the clean diamond C(110) surface slab. In the study of this initial series, tooltips were moved only along the z -coordinate with no tooltip tilting, rotation, or forced lateral movements of any kind. As in previous work,⁵ the clean diamond C(110) surface slab was constructed of 4 layers of carbon with the bottommost carbon layer terminated by hydrogen atoms. The model consisted of 160 carbon atoms and 40 hydrogen atoms and was confined to a periodic box with supercell dimensions of 14.245 \AA and 12.604 \AA along the edges surrounding the surface plane. The bottommost carbon layer and terminating hydrogen atoms of the surface slab were fixed in bulk-like positions during the simulations, with the z -coordinate defined as perpendicular to the surface.

A series of total energy minimization calculations were carried out to model the C_2 deposition process using the Si/Ge/Sn-based dimer placement tool, a 46-atom molecule consisting of 42 C and H atoms arranged in a fused triadamantane cage, plus 2 additional C atoms in the bound C_2 dimer and 2 atoms of Si, Ge, or Sn as the dimer-supporting atoms. Initially the toolbound carbon dimer was aligned with the ideal position of the global minimum (GM) of one ad-dimer on the clean C(110) surface. Subsequent tooltip steps were controlled in $0.1\text{--}0.2\text{ \AA}$ increments by fixing the positions of six hydrogen atoms on the topmost 6 carbon atoms of the tool, a constraint used in all later simulations. The lowest total energy configuration of the deposition process was then taken as the starting point for stepwise tool retraction AIMD simulations. The combined stepwise deposition/retraction AIMD simulations were performed for most tasks in this study. All the calculations were based on Density Functional Theory (DFT) with the generalized gradient approximation (GGA) and performed using the Vienna *Ab initio* Simulation Package (VASP).⁸ The present stepwise AIMD simulations employed a time step of 1 fs and a simulation time at each step of 200 fs, which is longer by a factor of 4–6 than the stretching time per vibration of the bonds in the ROI (vs only a 25 fs simulation time at each step in the prior work⁵). The present work also used a $0.1\text{--}0.2\text{ \AA}$ tool movement step size ($<10\%$ stretched bond length) in the vertical direction. Choosing these parameters allowed completion of approximately 4 fs of AIMD simulations per hour of elapsed computing time on 10 nodes of the in-house cluster computer, or approximately 55 hours per tool step.

Besides the electronic structure and stepwise AIMD calculations described above, we conducted several

longer-term classical molecular dynamics simulations on extended tooltip + handle complexes to deduce the thermal fluctuations in the normal modes of the attached carbon dimer, and the resulting dimer positional uncertainties as projected onto the plane of the diamond surface and also in the out-of-plane direction. These simulations were carried out for two representative extended tooltip handle structures at various temperatures using the modified MM2 (MM+, HyperChem 7.0)⁹ molecular mechanics force field.

3. RESULTS AND DISCUSSION

3.1. Isolated Dimer Placement on Clean Diamond C(110) Surface

This section reports results from numerous stepwise AIMD simulations of the deposition of carbon dimers onto the clear diamond C(110) surface using Si- and Ge-triadamantane dimer placement tools, and one stepwise AIMD simulation and a brief series of electronic structure geometry optimization calculations of dimer deposition onto C(110) using an Sn-triadamantane dimer placement tool.

3.1.1. Si Tool

Figure 1(A) shows the initial configuration for the stepwise AIMD retraction simulations of the Si-triadamantane dimer placement tool on clean diamond C(110) surface. The tool was raised stepwise from the surface in 0.2 Å increments to perform the retraction.

For Si tooltip operation at 300 K, Figure 1(B) shows the tool-dimer-surface ending configuration after 200 fs of

constant NVT simulation at the step height of 1.6 Å above the starting position. One carbon atom of the C₂ ad-dimer has pulled away from the surface when the tool was raised, indicating an undesired tooltip reaction.

To test our assumption that a 0.2 Å tool step size is small enough not to affect the phenomenon of interest, we performed a Si tool stepwise AIMD retraction simulation using a tenfold smaller tool step size of 0.02 Å with 200 fs constant NVT simulation at 300 K at each step. The Si tool retraction was started from a position 2.0 Å above the surface plane with the tool-bound dimer bonded to the C(110) surface. Beginning at 2.14 Å above the surface and continuing through 2.24 Å, one end-carbon of the ad-dimer was pulled away from the surface in the same manner as it happened at a height of 2.4 Å above the surface plane during the previous 0.2 Å tool step size simulation, thus supporting the validity of our 0.2 Å tool step size assumption.

To test possible synchronization with the maximum bond stretching at the last moment of a retraction step during our stepwise simulations, we performed a Si tool stepwise AIMD retraction simulation using the same parameters as previously employed but a longer simulation time of 300 fs at each step. The Si tool retraction was started from a position 1.8 Å above the surface plane with the tool-bound dimer bonded to the C(110) surface. At 2.6 Å above the surface plane, one end-carbon of the ad-dimer was pulled away from the surface in the same manner as it happened at a height of 2.4 Å above the surface plane during the previous calculations of 200 fs simulation at each step, thus supporting the validity of our adoption of 200 fs simulation time at each step—although the C(surface)–C(ad-dimer) bond breakage occurred at the opposite end of the ad-dimer.

A combined stepwise deposition/retraction AIMD simulation at 300 K for the Si-triadamantane dimer placement tool showed the same outcome as the retraction-only simulation. In the starting configuration, the carbon dimer was bound on the tooltip and positioned 3.0 Å above the diamond C(110) surface. The tool was then lowered stepwise toward the surface using a 0.2 Å tool step size and a 200 fs simulation at each step. When the C₂ dimer reached a position 2.2 Å above the surface, after 200 fs of constant NVT simulation the C₂ dimer formed loose connections with the corresponding substrate surface carbon atoms. From this moment onward we pulled the tool upward, using a 0.1 Å tool step size and a 300 fs simulation at each step. At a position of 2.8 Å to 2.9 Å above the diamond surface, one carbon atom of the C₂ ad-dimer was pulled away from the surface, again indicating an uncontrollable tooltip.

For the stepwise AIMD simulation of Si tooltip at 80 K, Figure 1(C) shows the tool-dimer-surface ending configuration after 200 fs constant NVT simulation at the step of 1.8 Å above the starting position. In this case, the ad-dimer was left bonded to the surface in the desired global

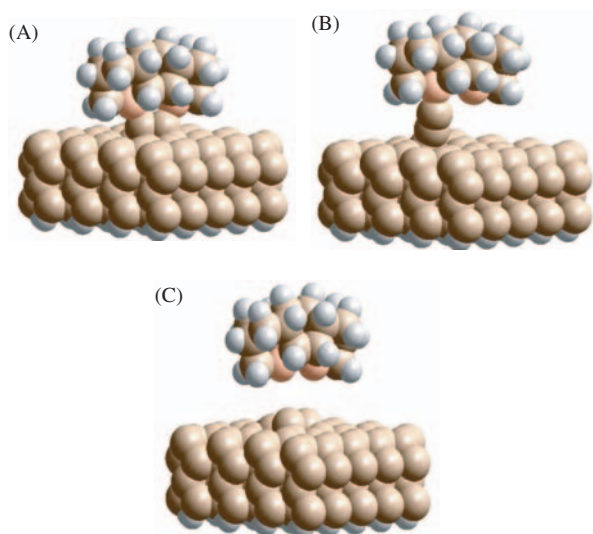


Fig. 1. Stepwise retraction simulation of Si-based tool from clean diamond C(110) surface: (A) initial configuration (C in brown, H in white, Si in orange); (B) ending configuration after 200 fs at 1.6 Å above starting position, at 300 K; (C) ending configuration after 200 fs at 1.8 Å above starting position, at 80 K.

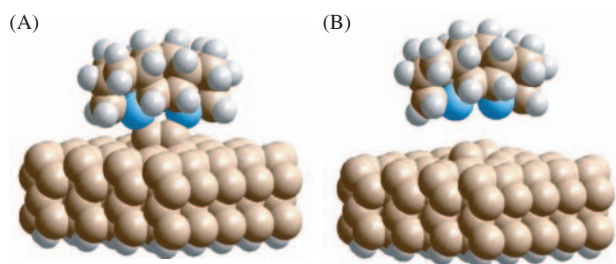


Fig. 2. Stepwise retraction simulation of Ge-based tool from clean diamond C(110) surface: (A) initial configuration (C in brown, H in white, Ge in blue); (B) ending configuration after 200 fs at 1.6 Å above starting position, at 300 K.

minimum configuration when the tool was raised, indicating a successful and controllable carbon dimer placement on C(110) surface with the Si tooltip at that temperature.

3.1.2. Ge Tool

Figure 2(A) shows the initial configuration for the stepwise AIMD retraction simulation of the Ge-triadamantane dimer placement tool on clean diamond C(110) surface. The tool was raised stepwise from the surface, using a 0.2 Å tool step size and a 200 fs constant NVT simulation at each step. Figure 2(B) shows the tool-dimer-surface ending configuration after 200 fs constant NVT simulation at the step of 1.6 Å above the starting position, at 300 K. In this case, the ad-dimer was left bonded to the surface in the desired global minimum configuration when the tool was raised, indicating a successful and controllable carbon dimer placement on C(110) surface.

The combined stepwise deposition/retraction AIMD simulation at 300 K for the Ge-triadamantane dimer placement tool showed the same outcome as the retraction-only simulation. In the initial configuration, shown in Figure 3(A), the carbon dimer was bound on the tooltip and positioned 3.0 Å above the diamond C(110) surface. The tool was then lowered stepwise toward the surface. Figure 3(B) shows the starting configuration of the system at the step of 2.4 Å above the surface, where the C₂ dimer on the tooltip had not yet significantly interacted with the diamond surface carbon atoms. After 200 fs of constant NVT simulation, the carbon dimer formed loose connections with the corresponding surface carbon atoms and the original bonds between the carbon dimer and the Ge atoms on the tooltip became weaker. This transitional configuration is captured in Figure 3(C). From this moment onward we pulled the tool upward within the usual stepwise retraction, resulting in the final separation of the carbon dimer from the tooltip and the subsequent adsorption of the C₂ ad-dimer onto the diamond surface. Figure 3(D) shows the ending system configuration after 200 fs constant NVT simulation when the tooltip has been raised to 0.8 Å above the transitional configuration. The ad-dimer was left bonded to the surface and relaxed to its global minimum

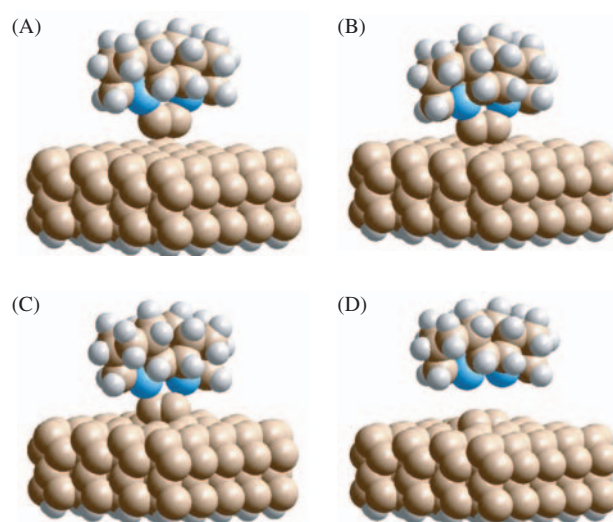


Fig. 3. Stepwise deposition/retraction simulation of Ge-based tool on clean diamond C(110) surface: (A) initial configuration, toolbound dimer positioned 3.0 Å above surface (C in brown, H in white, Ge in blue); (B) starting configuration at 0 fs at 2.4 Å above surface, at 300 K; (C) transitional configuration after 200 fs at 2.4 Å above surface, at 300 K; (D) ending configuration after 200 fs at 3.2 Å above surface, at 300 K.

(GM) arrangement, again indicating a successful and controllable room-temperature carbon dimer placement.

Note that the arrangement of the C₂ ad-dimer, which has connected to both tooltip and C(110) surface, calculated as the minimum energy configuration using deposition stepwise electronic structure calculations and shown in Figure 4, is similar to that of the local minimum configuration calculated for an isolated ad-dimer placed on the clean C(110) surface.⁴ For clarity, the tool frame was removed in Figure 4.

Finally, an additional stepwise AIMD retraction simulation of the Ge-triadamantane dimer placement tool was conducted using a 0.1 Å tool step size and a 300 fs constant NVT simulation at 300 K at each step, starting from the previously-described transitional configuration at

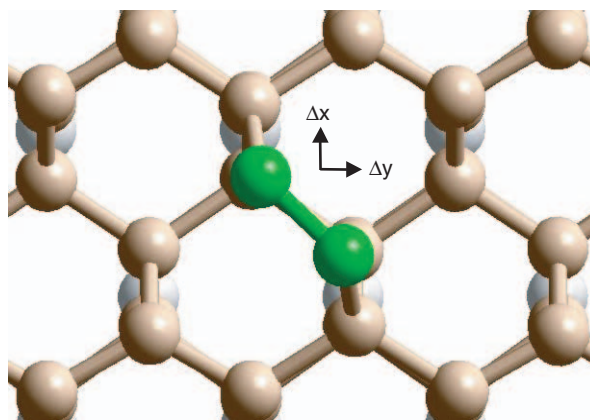


Fig. 4. Orientation of C₂ dimer (in green) in minimum energy configuration on the clean C(110) surface (C in brown, H in white) after deposition using Si- or Ge-based dimer placement tool.

a position 2.4 Å above the surface. As the stepwise retraction AIMD simulation proceeded from the step of 3.1 Å to 3.2 Å above the surface, the carbon ad-dimer detached from the tooltip and was left bonded to the diamond surface, gradually relaxing to the GM configuration as the tooltip lifted further, again indicating a successful and controllable carbon dimer placement at room temperature.

3.1.3. Sn Tool

The Sn-triadamantane dimer tool deposition and retraction from the clean diamond C(110) surface was modeled using stepwise geometry optimization calculations with 4 different sets of constraints on the top of the tooltip molecule, including (1) fixing xyz coordinates of the topmost 6 carbon atoms and their terminating H atoms, (2) fixing xyz coordinates of the topmost 2 carbon atoms, (3) fixing only the z coordinate of the topmost 2 carbon atoms, and (4) fixing only z coordinates of the topmost 10 carbon atoms, as well as varying the conditions of reducing step size in the transitional region from 0.1 Å to 0.01 Å for modeling the retraction and using higher convergence criterion for optimizing the wavefunction of the system. The results of all sets of geometry optimization scans showed that the Sn-triadamantane dimer placement tool successfully deposited the carbon dimer on the C(110) surface as the tool was retracted from the surface. However, after releasing the ad-dimer the discharged tooltip did not restore to its global minimum configuration but rather adopted a higher energy asymmetric structure.

Extensive room-temperature AIMD simulations of the Sn tool have not yet been done. However, one stepwise AIMD deposition-retraction simulation of the Sn tooltip at 300 K, using a 0.2 Å tool step size and a 200 fs constant NVT simulation at each step, found that the ad-dimer begins interacting with the surface at a height of 1.2 Å above it (Fig. 5(A)). During retraction the terminal Sn atoms are prone to attraction towards the surface carbon atoms. In the AIMD simulation, the Sn atoms displaced slightly toward the surface at 1.8 Å above it, the tip distorted seriously at 2.0 Å (Fig. 5(B)), and by 2.4 Å one of the Sn atoms had detached from the tooltip to reside on the deposition surface near the dimer (Fig. 5(C)). This suggests that C–Sn bonds might be too weak to permit a viable Sn-based tooltip design within the DCB6 tooltip family.

3.2. Placement of Adjacent Second Dimer on Clean C(110) Surface

This section reports results from two stepwise AIMD simulations of the deposition of a second carbon dimer immediately adjacent to a previously-placed isolated C₂ dimer within a trough of a clean diamond C(110) surface. In the first simulation, a combined stepwise deposition/retraction simulation at 300 K for the Ge-triadamantane dimer

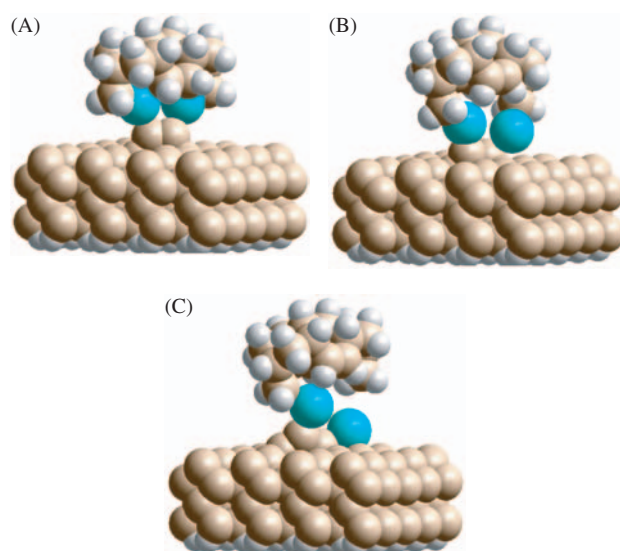


Fig. 5. Stepwise deposition/retraction simulation of Sn-based tool on clean diamond C(110) surface: (A) starting deposition configuration (to begin retraction), toolbound dimer positioned 1.2 Å above surface (C in brown, H in white, Sn in cyan); (B) transitional configuration after 200 fs at 2.0 Å above surface, at 300 K; (C) ending configuration after 200 fs at 2.4 Å above surface, at 300 K.

placement tool was begun after preparing the model structures by running geometry optimizations of the clean C(110) surface slabs with one ad-dimer. In the starting configuration, the carbon dimer was bound on the tooltip and initially positioned 3.0 Å above the diamond C(110) surface with the corresponding ideal lattice orientation, then moved vertically using a 0.2 Å tool step size and a 200 fs constant NVT simulation at each step. Upon lowering the tooltip to 2.8 Å above the surface, the second dimer formed bonds to the first dimer and to the surface. However, the second dimer did not relax to its GM arrangement even after the tooltip had retracted 4.9 Å from it, instead leaving the far-end carbon of the ad-dimer equilibrated about 3.1 Å away from the corresponding carbon atom of substrate, as compared to a distance of 1.6 Å if the GM arrangement had been reached. The second simulation was carried out with the tooltip 0.3 Å farther from the previously-placed C₂ dimer along the y -axis. The outcomes were similar, with the ad-dimer not having relaxed to the GM arrangement even after the tip was retracted to 5.5 Å above it. Until future research can reveal a misplacement-free approach trajectory, adjacent dimer placement on C(110) using the DCB6Ge tool must be regarded as a defect-prone process.

3.3. Placement of Gapped Second Dimer on Clean C(110) Surface

This section reports results from stepwise AIMD simulations of the deposition of a second isolated carbon dimer near a previously-placed isolated C₂ dimer such that the two ad-dimers have a one-dimer gap between them, again

within a trough of a clean diamond C(110) surface. A combined stepwise deposition/retraction simulation at 300 K for the Ge-triadamantane dimer placement tool was begun after preparing the model structures by running geometry optimizations of the clean C(110) surface slabs with one ad-dimer and two ad-dimers. In the starting configuration, the carbon dimer was bound on the tooltip and positioned 3.0 Å above the diamond C(110) surface, whereupon the tooltip was lowered stepwise toward the surface using a 0.2 Å tool step size and a 200 fs constant NVT simulation at each step. The calculations resulted in the same outcome for the second ad-dimer (i.e., a successful deposition) as in the simulation of the first isolated dimer deposition/retraction using the Ge tooltip (Section 3.1.2), including the transitional configuration formed at the step of 2.4 Å above the surface.

3.4. Dimer Intercalation Between Gapped Dimers on Clean C(110) Surface

Previous work found that if a single carbon dimer is positionally deposited within a trough of a clean diamond C(110) surface, the dimer easily relaxes to the global minimum structure.⁴ However, the two-dimer cluster formed by positioning a second carbon dimer adjacent to an isolated dimer in its global minimum can adopt one of 19 undesired local energy minima, five of which must traverse barriers >0.5 eV to reach the global minimum and thus constitute stabilized defects relative to the desired lattice structure. That is, placing C₂ dimers, one immediately next to the other, is prone to defect formation (Section 3.2).

To avoid this difficulty, we examined possible defect states available to a C₂ dimer intercalated between two previously-placed isolated C₂ dimers having a one-dimer gap between them, again within a trough of a clean diamond C(110) surface. After optimizing the global minimum structure of the two initial ad-dimers, which had the same configurations, a third C₂ ad-dimer was positioned parallel to the C(110) surface (consistent with the rigidity of the dimer placement tool) and was intercalated into the gap from various heights at 5 representative rotational angles (0°, ~ ±45°, ~ ±90°) around the center of the blank spot without in-plane rotational constraints. The energy minimization calculations showed that the third ad-dimer relaxed from all five initial orientations to just one local minimum, a metastable state, at the position about 1.2 Å above the two previously-placed isolated C₂ dimers (Fig. 6). The metastable 3-dimer cluster then converted to the desired global minimum (Fig. 7) by passing through a transition state with a barrier of only +0.22 eV (about 5 kcal/mole). The barrier height was determined using a series of partial optimization calculations in which the ad-dimer *z*-coordinate was restrained to progressively decrease in 0.01 Å step size from LM to GM. No local minima leading to defect configurations were found. This suggests a possible procedure for

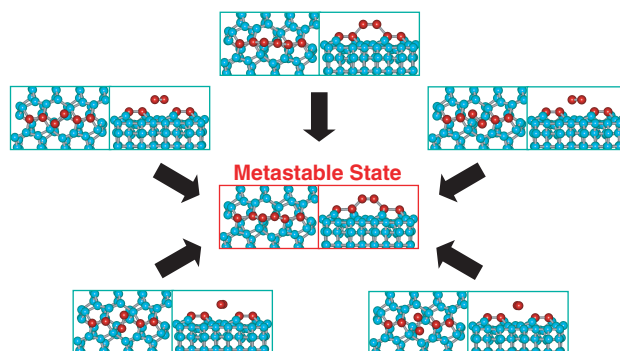


Fig. 6. Third C₂ dimer, intercalated into the gap between two C₂ dimers previously deposited on C(110) at various rotational angles, converges to a single metastable state.

positional dimer deposition that minimizes accessibility to defect states, wherein C₂ dimers are initially placed in every other position, rather than immediately adjacent, during the first pass, after which the blank spots between each existing pair of ad-dimers in a row are filled with ad-dimers during the second pass.

A stepwise AIMD simulation was conducted to test this procedure. In the starting configuration the carbon dimer was bound on the tooltip with the same orientation as in the metastable state and positioned 4.0 Å above the diamond C(110) surface. The tool was then lowered stepwise toward the surface. When the C₂ dimer reached a position 3.4 Å above the surface, after 200 fs constant NVT simulation at 300 K the C₂ dimer formed loose connections with the corresponding proximal carbon atoms of the previously deposited two ad-dimers, simultaneously weakening the original bonds between the tool-bound carbon dimer and the Ge atoms on the tooltip. After lifting the tool upward in the usual stepwise retraction from this point, the final separation of the carbon dimer from the tooltip and the subsequent adsorption of the C₂ ad-dimer onto the diamond surface occurred at a height of 4.2 Å above the

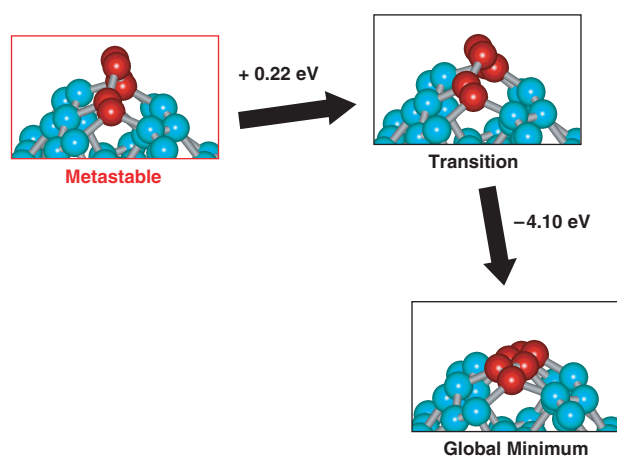


Fig. 7. Low barrier from local minimum (metastable state) to transition state, relaxing to global minimum, for third C₂ dimer intercalated into the gap between two C₂ dimers previously deposited on C(110).

surface after 200 fs constant NVT simulation at 300 K, whereupon the carbon dimer relaxed to its global minimum arrangement between the previously deposited 2 carbon ad-dimers. Thus a dimer deposition procedure directed first to producing gapped sites, then to filling the gaps, can successfully deposit fully populated dimer rows on C(110) surface.

3.5. Dimer Misalignment Tolerance During Placement on Clean C(110) Surface

To specify an experimental protocol to achieve practical diamond mechanosynthesis it is necessary to determine the maximum tolerable dimer misplacement error that will still result in a positionally correct C_2 deposition onto the diamond C(110) surface, either as an isolated ad-dimer or as an intercalation between two gapped dimers. For these studies, the xyz coordinate directions are defined the same as for the C(110) surface slab and do not refer to a tool-centered coordinate frame: The x -coordinate is perpendicular to the C(110) surface troughs, the y -coordinate is parallel to the troughs, and the z -coordinate is normal to the surface plane. This set of directions is adopted because the alignment of tools in practical operations will most probably refer to the coordinate frame of the substrate. Two principal classes of placement misalignment error are identified—rotational and translational.

3.5.1. Rotational Misalignment During Isolated Dimer Placement

In rotational placement error, the C_2 dimer may approach the target placement site rotated within the horizontal plane parallel to the diamond surface at some angle relative to the ideal lattice orientation for deposition. Rotational placement error may consist of an uncertainty component and a displacement component.

Regarding the uncertainty component, a diamond AFM tip is torsionally stiff, so the primary source of horizontal rotational uncertainty will be thermal vibrations of the tooltip-bound dimer. A 1-ps 300 K molecular mechanics simulation of the extended tool⁵ found the maximum in-plane rotation of a tool-attached dimer to be less than $\pm 8^\circ$ with an average of $\pm 2^\circ$. This represents a 0.04–0.16 Å displacement in the horizontal plane which is well within even the most conservative defect-avoidance placement accuracy of 0.2–0.5 Å,⁴ and also within the room-temperature tool-handle thermal uncertainties for all tools (Section 3.6).

As for the displacement component of the horizontal rotational placement error, the rotational allowance of placing an isolated carbon dimer on the clean C(110) surface was examined for the simplest case in which the rotational deviation is around the center of and with respect to the LM1 (single-dimer local minimum)⁴ position. The clockwise (CW) rotation viewed from the top was defined

as “minus” and the counterclockwise (CCW) rotation as “plus.” As in previous AIMD simulations, the 6 terminating hydrogen atoms which are bound to the topmost 2 carbon atoms and their neighboring 4 carbon atoms in the tooltip were fixed. During the stepwise AIMD simulations of deposition, trial CW rotations of -30° , -32.5° , and -35° and a trial CCW rotation of $+30^\circ$ yielded controllable behavior, whereas CCW rotations of $+32.5^\circ$, $+35^\circ$, $+45^\circ$, and $+60^\circ$ resulted in defect formation. During the stepwise AIMD simulations of retraction, a trial CW rotation of -30° and a trial CCW rotation of $+30^\circ$ left the carbon dimer bonded to the surface, relaxed to its global minimum arrangement, whereas CW rotations of -32.5° and -35° and CCW rotations of $+32.5^\circ$ and $+35^\circ$ resulted in uncontrollable behavior. Thus stepwise AIMD predicts the maximum horizontal rotational allowance of the Ge tool is -30° to $+30^\circ$ for adding a single isolated carbon dimer to C(110).

A related source of possible placement error might occur when the tooltip is rolled to some intermediate angle relative to the vertical (such that the vertical tool axis is no longer perpendicular to the deposition plane) while maintaining the toolbound C_2 dimer parallel to LM1 in the horizontal plane, as previously described for single-dimer depositions on C(110). Tip rolling is likely to be required in practical situations where a dimer must be delivered to a side position (e.g., a vertical face) on a workpiece rather than to a top position, or where two tooltips must operate in close proximity near a workpiece and it becomes necessary to tilt both tools away from vertical to reduce steric congestion. The simplest case is where the tool is first oriented with the C_2 dimer parallel to LM1 as if in preparation for a single-dimer deposition on C(110), but the tool is then rotated through some angle θ_{roll} around an axis defined by the line connecting the two carbon dimer atoms on the tip. After such tilting, the tool is subsequently moved only in the z direction, as before. During deposition, the dimer will still approach the C(110) surface with the dimer axis parallel to the xy surface plane, but the tool will now be tilted to the C(110) surface, not normal to it. Stepwise AIMD simulations of the Ge tool placed in this tilted orientation at 300 K found that the tool still deposits the dimer successfully on the C(110) surface at $\theta_{\text{roll}} = 30^\circ$ and 32.5° , but shows uncontrollable behavior at $\theta_{\text{roll}} = 35^\circ$, giving a maximum tolerable “in-plane” tip rolling angle of $\theta_{\text{roll, max}} = 32.5^\circ$.

Another rotational placement error is the case where the C_2 dimer which is attached to the tooltip arrives at the diamond surface no longer parallel to the horizontal plane. Here again, the vertical rotational placement error may consist of an uncertainty component and a displacement component.

Regarding the uncertainty component, a 1-ps 300 K molecular mechanics simulation of the extended tool⁵ found the maximum out-of-plane rocking angle of a tool-attached dimer due to thermal motions to be less than $\pm 5^\circ$

with an average of $\pm 1^\circ$. This represents a 0.02–0.10 Å displacement in the vertical direction which is within the room-temperature tool-handle z -axis thermal uncertainties for all tools (Section 3.6).

As for the displacement component, state-of-the-art nanopositioners such as the PicoCube™ from Physik Instrumente typically introduce minimal off-axis displacement-from-vertical tilts of only $<1 \mu\text{rad}$ ($<0.0001^\circ$). Nevertheless, the sensitivity of dimer placement to tooltip rocking (wagging) motions was investigated using stepwise AIMD simulations of the Ge tool placed in this tilted orientation at 300 K. These simulations found that the tool still deposits the dimer successfully on the C(110) surface at a rocking angle $\theta_{\text{rock}} = 15^\circ$ but shows uncontrollable behavior at $\theta_{\text{rock}} = 17.5^\circ$ and 20° , giving a maximum tolerable “out-of-plane” tip rocking angle of $\theta_{\text{rock,max}} = 15^\circ$.

3.5.2. Translational Misalignment During Isolated Dimer Placement

In translational placement errors, the C_2 dimer may approach the target placement site at some linear displacement Δx and Δy (lattice directions defined in Fig. 4) from the ideal lattice position for deposition on the diamond C(110) surface. The uncertainty component is described in Section 3.6. To investigate the displacement component of the translational x - and y -coordinate dimer misplacement tolerance using the Ge tool, a series of stepwise AIMD deposition/retraction simulations using 0.15 Å (deposition phase) or 0.20 Å (retraction phase) tool step sizes and a 200 fs constant NVT simulation at 300 K at each tool step were performed with the tool displaced by various increments in x and y from the corresponding ad-dimer local minimum energy (LM1)⁴ arrangement (Fig. 4).

For the translational x -coordinate dimer misplacement tolerance using a Ge tool, during deposition phase of the stepwise AIMD simulations, the toolbound dimer formed the desired bonding with C(110) surface for x -coordinate deviations of 0.5 Å, 0.7 Å, and 0.8 Å, whereas defect states occurred at x -coordinate deviations of 0.9 Å and 1.0 Å. During retraction phase, stepwise AIMD simulations for x -coordinate deviations of 0.6 Å, 0.7 Å, and 0.8 Å revealed uncontrollable behavior with one end carbon of the placed dimer pulled away from the substrate while raising the tip. The stepwise AIMD simulation with x -coordinate deviation of 0.5 Å revealed that the ad-dimer was left bonded on the substrate and relaxed to its GM arrangement. Thus the maximum x -coordinate dimer misplacement tolerance at 300 K using the Ge dimer placement tool for isolated C_2 placement on clean C(110) is 0.5 Å.

For the translational y -coordinate dimer misplacement tolerance using a Ge tool, during deposition phase of the simulations, the toolbound dimer formed the desired bonding with C(110) surface for y -coordinate deviations of 0.5 Å, 0.7 Å, 0.9 Å, 1.0 Å, and 1.1 Å. During retraction

phase, the simulation for y -coordinate deviation of 1.1 Å revealed uncontrollable behavior with one end carbon of the placed dimer pulled away from the substrate while raising the tip, but simulations for y -coordinate deviations of 0.5 Å, 0.7 Å, 0.9 Å, and 1.0 Å showed successful ad-dimer placement. Thus the maximum y -coordinate dimer misplacement tolerance at 300 K using the Ge dimer placement tool for isolated C_2 placement on clean C(110) is 1.0 Å.

3.5.3. Rotational Misalignment During Intercalated Dimer Placement

Rotational positional placement errors may occur during the intercalation of a dimer between two gapped dimers previously deposited on the clean diamond C(110) surface. Rotational placement uncertainties in the horizontal plane and thermally-induced dimer rocking (z -axis tilt) misalignments should be relatively small and well-tolerated (Section 3.5.1). As already noted (Section 3.4), a third free-rotating C_2 ad-dimer positioned parallel to the C(110) surface and intercalated between two gapped dimers at 5 representative rotational angles (0° , $\sim \pm 45^\circ$, $\sim \pm 90^\circ$) relaxed from all five initial orientations to just one local minimum, then converted to the desired global minimum through a low energy barrier.

The displacement component of the horizontal rotational placement error for dimer intercalation was investigated in the same way as previously described for isolated dimer placement in Section 3.5.1, but the rotational deviation was around the center of, and with respect to, the metastable state arrangement. During the stepwise AIMD simulations of deposition, CW rotations of -10° , -12.5° , -15° , -17.5° , -20° , -22.5° , -25° , and -30° and CCW rotations of $+20^\circ$ and $+22.5^\circ$ yielded controllable behavior, whereas CCW rotations of $+25^\circ$ and $+30^\circ$ resulted in defect formation. During the stepwise AIMD simulations of retraction, CW rotation of -10° and CCW rotations of $+20^\circ$ and $+22.5^\circ$ yielded a carbon dimer bonded to the surface, relaxed to its global minimum arrangement, whereas CW rotations of -12.5° , -15° , -17.5° , -20° , -22.5° , -25° , and -30° resulted in uncontrollable behavior. Thus stepwise AIMD predicts the maximum horizontal rotational allowance of the Ge tool is -10° to $+22.5^\circ$ for intercalating a dimer between two gapped dimers on C(110).

3.5.4. Translational Misalignment During Intercalated Dimer Placement

Translational positional placement errors may also occur during the intercalation of a dimer between two gapped dimers previously deposited on the clean diamond C(110) surface.

To investigate the translational x -coordinate dimer misplacement tolerance using the Ge tool, the tool-bound

dimer was first aligned above the position in the intercalated ad-dimer metastable state structure, along the x and y directions. Then a series of downward stepwise geometry optimization calculations was performed on the system after augmenting the x -coordinate by 1.0 Å, starting from an initial height of 2.4 Å above the two previously-deposited gapped ad-dimers using a 0.10 Å step size. At the height of 2.0 Å above the gap, the tip-bound C₂ dimer interacted with the proximal carbon atoms of the two gapped ad-dimers already on the surface. Similar downward stepwise geometry optimization calculations, performed after augmenting the x -coordinate by 1.5 Å and using a 0.10 Å step size, found that at the height of 1.7 Å above the gap, the tip-bound C₂ dimer again interacted with the desired proximal carbon atoms of the two gapped ad-dimers on the surface.

This was followed by a series of stepwise AIMD deposition/retraction simulations using a 200 fs simulation time at each step and a 0.15 Å tool step size with the Ge tool at 300 K, starting from an initial height of 2.0 Å above the two previously-deposited gapped ad-dimers and an x -coordinate deviation of 1.5 Å. After 200 fs simulation at the step of 1.85 Å above the gap, one end of the tool-bound C₂ dimer left the tip and inserted between a proximal carbon atom of one of the two ad-dimers and the adjacent carbon atom in the substrate (breaking the bond between them, then forming bonds with them, respectively)—a significantly different result from the previous 0 K electronic structure calculation. Stepwise AIMD simulation with 1.4 Å x -coordinate deviation started from the height of 2.10 Å above the gap showed the same tendency of uncontrollability. The stepwise AIMD simulation with 1.3 Å x -coordinate deviation revealed uncontrollable behavior in the retraction phase such that one end of the tip-bound C₂ dimer was pulled far away from the proximal carbon atoms of the two gapped ad-dimers on the surface. A 1.2 Å x -coordinate deviation yielded a controllably surface-bonded dimer, but the dimer would not assume the global minimum arrangement even after full tool retraction, and a 1.1 Å x -coordinate deviation likewise showed uncontrollable behavior with one end of the placed carbon dimer pulled away from the substrate during retraction. Stepwise AIMD simulation with 1.0 Å x -coordinate deviation confirmed the desired interaction with the gapped ad-dimers at 2.15 Å above the gap during the deposition phase, and after retraction to 2.95 Å above the gap the carbon dimer relaxed to the global minimum arrangement. Thus the maximum x -coordinate dimer misplacement tolerance at 300 K using the Ge dimer placement tool for C₂ intercalation between two gapped ad-dimers on clean C(110) is 1.0 Å.

To investigate the translational y -coordinate dimer misplacement tolerance using the Ge tool, the tool-bound dimer was again initially aligned to the ad-dimer position in the intercalated metastable state structure along the

x and y directions. A downward stepwise geometry optimization calculation on this system showed a tendency of uncontrollability for y -coordinate augmentations of 1.0 Å and 0.6 Å at a height of 2.3 Å above the gapped ad-dimers. A similar calculation for smaller y -coordinate augmentations of 0.5 Å and 0.4 Å predicted that the tool-bound C₂ dimer interacted with the desired proximal carbon atoms of the two gapped ad-dimers on the C(110) diamond surface, at a height of 2.2 Å above the gapped ad-dimers.

This was followed by a series of stepwise AIMD deposition/retraction simulations using a 200 fs simulation time at each step and 0.10 Å (deposition) or 0.15 Å (retraction) tool step sizes with the Ge tool at 300 K, starting from an initial height of 2.4 Å above the two previously-deposited gapped ad-dimers and a y -coordinate deviation of 0.8 Å and 0.7 Å, both of which showed the same tendency of uncontrollability during the deposition phase at a height of 2.3 Å above the gapped ad-dimers. Stepwise AIMD on a 0.6 Å y -coordinate deviation showed the desired interaction with the gapped ad-dimers during deposition, but the tool retraction became uncontrollable at the step of 2.65 Å above the gapped ad-dimers, as did the retractions on a 0.5 Å and a 0.4 Å y -coordinate deviation at the step of 2.80 Å above the gapped ad-dimers. On 0.3 Å y -deviation during the retraction phase the dimer was deposited on the surface in its global minimum energy position after the Ge tip had pulled clear of the surface at the step of 3.20 Å above the original gap. Thus the maximum y -coordinate dimer misplacement tolerance at 300 K using the Ge dimer placement tool for C₂ intercalation between two gapped ad-dimers on clean C(110) is 0.3 Å.

Note that for x deviations (across trough), the maximum tolerable dimer misplacement error is 0.5 Å for an isolated C₂ deposition but 1.0 Å for C₂ intercalation between two gapped ad-dimers, indicating that a much larger placement error is tolerable for the intercalation approach. For y deviations (along trough), the maximum tolerable dimer misplacement errors give the opposite results, with 1.0 Å for an isolated C₂ deposition and 0.3 Å for C₂ intercalation between two gapped ad-dimers. However, misplacement errors for the two modes of deposition (isolated vs intercalated) are not strictly comparable because during an isolated C₂ deposition the tooltip-bound carbon dimer is aligned in the xy plane to the LM1 position,⁴ in which the ad-dimer is parallel to neither x nor y directions, whereas during C₂ intercalation between two gapped ad-dimers the tooltip-bound carbon dimer is aligned in the xy plane to the metastable state position (when it starts interacting with the targeted carbons on C(110)), in which the ad-dimer becomes parallel to the troughs (y direction).

3.6. Thermal Uncertainty of Handle-Mounted Tooltips

Extending the exploration of temperature effects on the positional uncertainty and control of the terminal carbon dimer first reported in Part II,⁵ a series of MD simulations

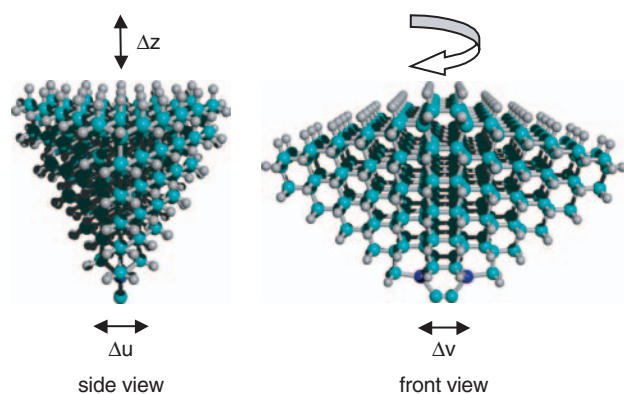


Fig. 8. Side view (left) and front view (right) of extended Geriadamantane dimer placement tool for diamond mechanosynthesis (C in cyan, H in white, Ge in blue).

of the original Si-, Ge-, and Sn-based 430-atom extended diamond tooltip handle structure (Fig. 8) were conducted using simulation run times of sufficient length to compute the phase space distribution of the positions and momenta of the terminal carbon dimer atoms. The original tooltip handle structure shown in Figure 8 is narrower, hence less stiff against transverse displacements, in the u -direction normal to the dimer axis than in the v -axis parallel to the dimer axis. Initial independent 100 ps simulations of the Ge tool at 80 K and 300 K, whether using 4 or 50 tooltip restraint atoms, or small or large tether forces, all developed significant (approx. ± 2 Å) u -axis ~ 2 THz oscillations, beginning after ~ 20 ps into the simulation, consistent with the estimated natural resonant frequency of a clamped diamond rod having dimensions similar to

those of the as-modeled extended tool handle (14.58 Å (u), 25.68 Å (v), 14.66 Å (z)). A simple continuum model¹⁰ using Bernoulli-Euler theory—with the extended tooltip handle crudely modeled as a clamped-free cylindrical beam of length $L = 1.4$ nm, equivalent circular cross-sectional radius $R \sim 0.7$ nm, Young's modulus $E = 1.05 \times 10^{12}$ N/m² and density $\rho = 3510$ kg/m³ for diamond, frequency mode constant $\beta_1 \sim 1.875$ for the lowest vibrational frequency mode ($i = 1$), and second moment of area $I = \pi R^4/4$ —gives the lowest natural resonant frequency as $\nu_1 = (\beta_1^2/4\pi)(R/L^2)(E/\rho)^{1/2} \sim 1.7$ THz. The artificial character of this resonance was confirmed by comparing a 300 K high-resolution 1 ps simulation at 1 fs data intervals of the Ge tool, yielding a resonance frequency estimate of 1.797 ± 0.005 THz over 2 cycles, to a 300 K high-resolution 1 ps simulation at 1 fs data intervals of a shortened Ge tool (14.55 Å (u), 21.53 Å (v), 12.49 Å (z)) having its topmost sheet of carbon atoms removed, yielding a resonance frequency estimate of 2.035 ± 0.023 THz over 2 cycles, a 13% increase in resonance frequency compared to the larger tool. A 19% decrease in cylindrical beam width along with a 17% reduced beam length, similar to the aforementioned size reduction in the Ge tool, would increase the estimated Bernoulli-Euler natural resonant frequency by $\sim ((R/L^2) - 1) \sim (((0.81)/(0.83)^2) - 1) \sim 17\%$, comparable to the observed 13% increase for the shortened Ge tool, confirming that the resonance is most likely a modeling artifact.

By cumulating data from a series of independent 5 ps or 10 ps MD simulations until the positional extremum values and standard deviations (σ) remained unchanged to

Table I. Molecular dynamics evaluation of carbon dimer atom maximum positional uncertainty and standard deviation of positional uncertainty in a DCB6-X (X = Si, Ge, Sn) tooltip molecule1 bound to extended diamond tooltip handles, as a function of temperature.

| Tool temperature $T(K)$ | Tooltip type | Total simulation time (ps) | Uncertainty Δu and $(3\sigma_u)$, in Å | Uncertainty Δv and $(3\sigma_v)$, in Å | Uncertainty Δz and $(3\sigma_z)$, in Å |
|-------------------------|--------------|----------------------------|---|---|---|
| 20 | Si | 10 | ± 0.11 (0.14) | ± 0.03 (0.03) | ± 0.05 (0.06) |
| | Ge | 70 | ± 0.17 (0.14) | ± 0.07 (0.06) | ± 0.05 (0.04) |
| | Sn | 30 | ± 0.19 (0.19) | ± 0.04 (0.03) | ± 0.05 (0.06) |
| 80 | Si | 30 | ± 0.23 (0.26) | ± 0.07 (0.07) | ± 0.17 (0.21) |
| | Ge (XBar) | 20 | ± 0.14 (0.17) | ± 0.07 (0.07) | ± 0.09 (0.09) |
| | Ge | 80 | ± 0.36 (0.31) | ± 0.15 (0.11) | ± 0.10 (0.09) |
| | Sn | 30 | ± 0.35 (0.32) | ± 0.09 (0.08) | ± 0.10 (0.10) |
| 300 | Si (XBar) | 50 | ± 0.33 (0.30) | ± 0.15 (0.12) | ± 0.17 (0.18) |
| | Si | 60 | ± 0.40 (0.37) | ± 0.16 (0.14) | ± 0.16 (0.14) |
| | Si (II) | 10,000 | ± 0.35 (0.20) | ± 0.21 (0.12) | ± 0.17 (0.10) |
| | Ge (XBar) | 40 | ± 0.28 (0.30) | ± 0.15 (0.13) | ± 0.17 (0.15) |
| | Ge | 90 | ± 0.57 (0.50) | ± 0.15 (0.15) | ± 0.20 (0.19) |
| | Ge (II) | 10,000 | ± 0.52 (0.31) | ± 0.28 (0.21) | ± 0.30 (0.15) |
| | Sn (XBar) | 50 | ± 0.48 (0.48) | ± 0.18 (0.16) | ± 0.22 (0.18) |
| 900 | Sn | 30 | ± 0.61 (0.60) | ± 0.17 (0.15) | ± 0.23 (0.25) |
| | Si | 40 | ± 0.58 (0.54) | ± 0.33 (0.32) | ± 0.27 (0.26) |
| | Ge | 70 | ± 0.85 (0.78) | ± 0.43 (0.44) | ± 0.39 (0.30) |
| | Sn | 30 | ± 1.16 (1.08) | ± 0.32 (0.30) | ± 0.34 (0.32) |

XBar: values from present work with u -axis crossbar added to extended tool handle to improve handle stiffness.

II: values extracted or computed from original data⁵ for both dimer atoms.

within $\pm 0.01 \text{ \AA}$ upon addition of new data, the spatial distribution resulting from the normal high-frequency vibrational modes of each tool could be explored with minimal contributions from the artifactual THz resonance. Simulations were performed by tethering all 50 carbon atoms in the topmost plane of the tool handle to their energy-minimized positions using a large force restraint equal to the MM2 force field¹¹ C–C bond stiffness⁹ of 440 N/m, or 633 kcal/mol- \AA^2 , with different initial atomic positions and randomized initial velocities for each independent simulation using an integration time-step of 1 fs.

Table I summarizes the thermally-driven positional uncertainty of one of the two dimer carbon atoms, both in the dimer uv coordinate plane parallel to the xy plane of the diamond surface and in the out-of-plane (z -axis) direction, relative to its equilibrium position. Maximum positional uncertainty is conservatively defined as the extremum values observed along each coordinate axis during each series of simulations. These values are extracted from data sampled at 10 fs intervals at four representative

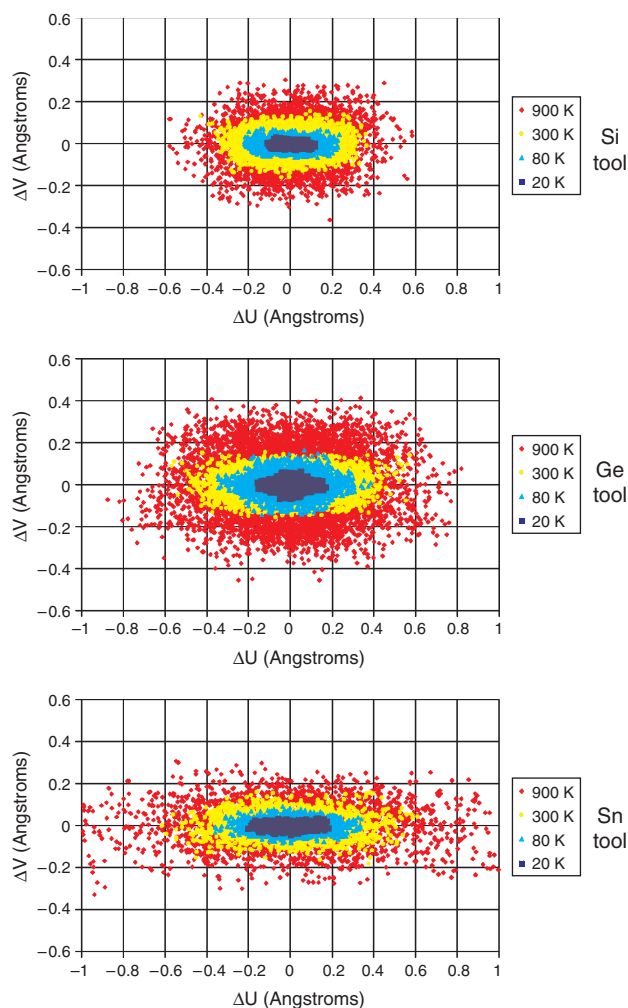


Fig. 9. Spatial distribution in horizontal uv -plane of one carbon in C_2 dimer on Si-, Ge-, and Sn-based triadamantane dimer placement tool mounted on original handle structure.

operating temperatures. The presumptive 3σ standard deviation of positional uncertainty (which would include 99.7% of all data if normally distributed) is given in parentheses in Table I, with data for the Si, Ge, and Sn tools plotted in Figure 9. For all three tools, dimer positional variance (σ^2) scales roughly with temperature (T) consistent with classical engineering approximations for thermally excited rods.³ Our results using MM+ at 300 K are quantitatively similar to those previously obtained by Mann et al.⁵ (“II” values, Table I) who used MM3 and hundred-fold longer simulation times. The significantly larger deviations in the atomic positions of the dimer carbon atom for the Ge tooltip as compared to the Si tooltip are due to the differences between the C–Si and C–Ge vibrational frequencies—stretching frequencies for isolated C–Si and C–Ge dimers are 905 cm^{-1} and 708 cm^{-1} , respectively,⁷ and $500\text{--}600 \text{ cm}^{-1}$ for C–Sn in various organotin(IV) complexes.^{12–14} A higher vibrational stretching frequency (as in C–Si) is characteristic of a stiffer bond which is less subject to large amplitude thermal fluctuations (and vice versa for lower frequency molecular vibrations). A design modification to the original extended tool handle suggested by Freitas (personal communication, 2004), intended to improve u -axis stiffness, is the addition of a u -axis crossbar structure (Fig. 10) which dramatically reduces u -axis positional uncertainty (“XBar” values, Table I) for the Ge tool, and to a lesser degree for the Sn and Si tools.

Data for just a single carbon dimer atom were deemed representative of the C_2 atom pair because the positional uncertainty statistics for the two dimer atoms in the loaded

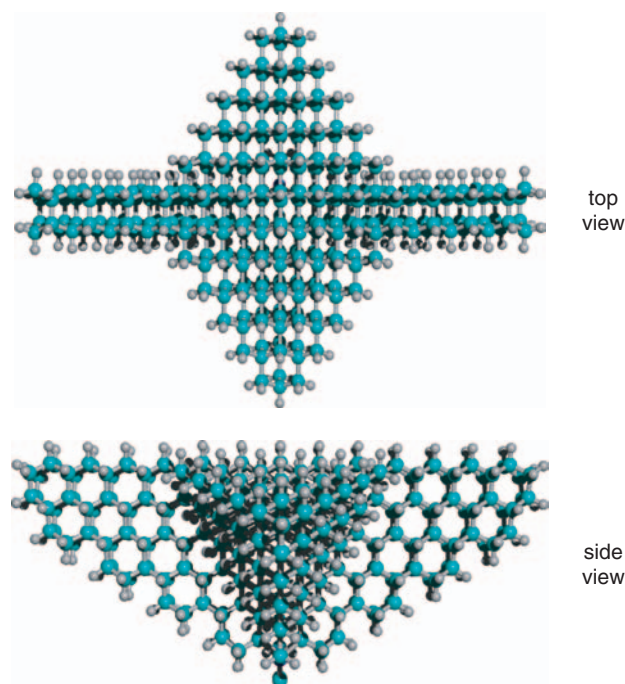


Fig. 10. Top and side views of crossbar tool handle for extended Ge-triadamantane dimer placement tool for diamond mechanosynthesis (C in cyan, H in white, Ge in blue).

tooltip are almost identical: $\Delta v_1 = \pm 0.20 \text{ \AA}$ ($3\sigma_{v1} = 0.13 \text{ \AA}$) for dimer atom 1 and $\Delta v_2 = \pm 0.21 \text{ \AA}$ ($3\sigma_{v2} = 0.12 \text{ \AA}$) for dimer atom 2 in the Si tool, and $\Delta v_1 = \pm 0.28 \text{ \AA}$ ($3\sigma_{v1} = 0.20 \text{ \AA}$) for dimer atom 1 and $\Delta v_2 = \pm 0.29 \text{ \AA}$ ($3\sigma_{v2} = 0.22 \text{ \AA}$) for dimer atom 2 in the Ge tool, at 300 K, according to raw data from Mann et al.⁵

4. CONCLUSIONS

The process of placing an isolated carbon dimer on diamond C(110) surface via the Si-substituted triadamantane dimer placement tool is unreliable at 300 K, but is reliable at 80 K. With the Ge-substituted triadamantane dimer placement tool, the process of placing an isolated C₂ dimer on the diamond C(110) surface is reliable at temperatures up to 300 K. The initial projected orientation on the diamond surface of the C₂ dimer transferred from the tooltip should be the same as that of the local minimum (LM1) of an isolated carbon ad-dimer placed on the same surface. The deposition of an isolated C₂ dimer on the diamond C(110) surface via the Sn-substituted triadamantane dimer placement tool appears unreliable.

Deposition of a second carbon dimer immediately adjacent to a previously-placed isolated C₂ dimer on C(110) is prone to defect formation. However, deposition on C(110) of a second isolated carbon dimer near a previously-placed isolated C₂ dimer such that the two ad-dimers have a one-dimer gap between them, using the Ge tool at 300 K, is predicted by stepwise AIMD simulation to result in the same outcome for the second ad-dimer as in the deposition simulation of the first isolated dimer.

Stepwise geometry optimizations of a free C₂ dimer, which is oriented at 0°, ~±45°, or ~±90° rotations in the horizontal plane around the center of a blank spot between two gapped previously-placed isolated C₂ ad-dimers, showed that the dimer relaxes from all five initial orientations to just one local minimum, a metastable state, then easily converts to the desired global minimum. This suggests a defect-reduced procedure for positional dimer deposition in which C₂ dimers are initially placed in every other position during the first pass, after which the blank spots between each existing pair of ad-dimers are filled with ad-dimers during the second pass. Stepwise AIMD predicts a controllable dimer intercalation between gapped dimers on clean C(110) surface using the Ge tool at 300 K via this procedure, yielding fully populated dimer rows.

Stepwise AIMD simulations quantify the maximum tolerable dimer misplacement error as 0.5 Å in *x* direction (across trough) and 1.0 Å in *y* direction (along trough) for a positionally-correct deposition of an isolated C₂ dimer on C(110), and 1.0 Å in *x* and 0.3 Å in *y* for C₂ intercalation between two gapped ad-dimers. Rotational misplacement tolerances for the Ge tool in the horizontal plane are -30° to +30° for adding a single isolated dimer to C(110) and -10° to +22.5° for intercalating a single dimer between two gapped ad-dimers, according to

stepwise AIMD simulations. For isolated dimer placement, the tool can tolerate a maximum “in plane” tip rolling angle of 32.5° and a maximum “out-of-plane” tip rocking angle of 15°, at 2.5° increments.

In this study, we performed 20 constant NVT stepwise AIMD simulations on the DCB6Ge carbon dimer placement tool at 300 K within the maximum tool misalignment errors. All simulations revealed successful placement of a carbon ad-dimer on the C(110) surface with various different initial settings. This indicates statistically that the DCB6Ge tooltip should work virtually all of the time to place a carbon dimer on the C(110) surface within the allowed range of tool misalignment, up to room temperature.

Thermal positional uncertainty of the tool-bound dimer is calculated using classical molecular dynamics for Si-, Ge-, and Sn-based dimer placement tools at operating temperatures of 20 K, 80 K, 300 K, and 900 K. At 300 K, maximum dimer placement uncertainty for the Ge tooltip + handle system is ±0.57 Å ($3\sigma = 0.50 \text{ \AA}$) along the narrow handle *u*-axis and ±0.15 Å ($3\sigma = 0.15 \text{ \AA}$) along the wide handle *v*-axis, in the horizontal plane, and ±0.20 Å ($3\sigma = 0.19 \text{ \AA}$) in the vertical *z*-axis. MD analysis of a new Ge tooltip + handle system at 80 K and 300 K finds that maximum dimer positional uncertainty is halved, e.g., from ±0.57 Å to ±0.28 Å at 300 K, by adding a crossbar in the most compliant *u*-axis direction. Total positional error is the sum of the dimer misplacement error and the thermal uncertainty of the tip.

References

1. Ralph C. Merkle and Robert A. Freitas, Jr., *J. Nanosci. Nanotechnol.* 3, 319 (2003).
2. C. D. Schaeffer, Jr., C. A. Strausser, M. W. Thomsen, and C. H. Yoder, Table 6. Common Bond Energies (*D*) and Bond Lengths (*r*), in *Data for General, Inorganic, Organic, and Physical Chemistry*, The Wired Chemist (1989); http://wulfenite.fandm.edu/Data/Table_6.html
3. K. Eric Drexler, *Nanosystems: Molecular Machinery, Manufacturing, and Computation*, John Wiley and Sons, New York (1992).
4. Jingping Peng, Robert A. Freitas, Jr., and Ralph C. Merkle, *J. Comput. Theor. Nanosci.* 1, 62 (2004).
5. David J. Mann, Jingping Peng, Robert A. Freitas, Jr., and Ralph C. Merkle, *J. Comput. Theor. Nanosci.* 1, 71 (2004).
6. T. Shimanouchi, *Natl. Stand. Ref. Data Ser. Natl. Bur. Stand. (USA)*, 1, 39 (1972).
7. Antonis N. Andriotis, Madhu Menon, and George E. Froudakis, *J. Cluster Sci.* 10, 549 (1999).
8. G. Kresse and J. Furthmuller, *Vienna Ab-Initio Simulation Package (VASP): The Guide*, VASP Group, Institut fur Materialphysik, Universitat Wien, Sensengasse 8, A-1130 Wien, Vienna, Austria (2003).
9. HyperCube, Inc., *HyperChem Computational Chemistry*, Publication HC70-00-04-00 (2002); MM2 (1991) parameter set (*runfiles/mmpstr.txt*) contributed by Norman Allinger.
10. Dong Qian, Gregory J. Wagner, Wing Kam Liu, Min-Feng Yu, and Rodney S. Ruoff, in *Mechanics of Carbon Nanotubes. Handbook of Nanoscience, Engineering, and Technology*, edited by William A. Goddard, III, Donald W. Brenner, Sergey Edward Lyshevski, and Gerald J. Iafrate, CRC Press, Boca Raton, FL (2003), pp. 19-1–19-63.

11. U. Burkert and N. L. Allinger, *Molecular Mechanics*, American Chemical Society, Washington, DC (1982).
12. Sadiq-ur-Rehman, Saqib Ali, Moazzam H. Bhatti, Khadija Shahid, M. Mazhar, M. Kaleem, and Amin Badshah, *Turk. J. Chem.* 26, 905 (2002). <http://journals.tubitak.gov.tr/chem/issues/kim-02-26-6/kim-26-6-12-0201-15.pdf>
13. L. Ronconi, C. Marzano, U. Russo, S. Sitran, R. Graziani, and D. Fregona, *Appl. Organometallic Chem.* 17, 9 (2003). <http://www.environmental-center.com/magazine/wiley/0268-2605/pdf2.pdf>
14. Mukta Jain and R. V. Singh, *Appl. Organometallic Chem.* 17, 616 (2003). <http://www3.interscience.wiley.com/cgi-bin/abstract/104537735/ABSTRACT>.

Received: 10 October 2005. Accepted: 7 November 2005.